



**HAL**  
open science

## Sol-gel engineering to tune structural colours

Marco Faustini

► **To cite this version:**

Marco Faustini. Sol-gel engineering to tune structural colours. Journal of Sol-Gel Science and Technology, 2020, 10.1007/s10971-020-05319-7 . hal-02895489

**HAL Id: hal-02895489**

**<https://hal.sorbonne-universite.fr/hal-02895489v1>**

Submitted on 9 Jul 2020

**HAL** is a multi-disciplinary open access archive for the deposit and dissemination of scientific research documents, whether they are published or not. The documents may come from teaching and research institutions in France or abroad, or from public or private research centers.

L'archive ouverte pluridisciplinaire **HAL**, est destinée au dépôt et à la diffusion de documents scientifiques de niveau recherche, publiés ou non, émanant des établissements d'enseignement et de recherche français ou étrangers, des laboratoires publics ou privés.

# Sol-gel engineering to tune structural colours

Marco Faustini<sup>1\*</sup>

<sup>1</sup>Sorbonne Université, CNRS, Collège de France UMR 7574 Chimie de la Matière Condensée de Paris, F-75005 Paris, France

[marco.faustini@sorbonne-universite.fr](mailto:marco.faustini@sorbonne-universite.fr)

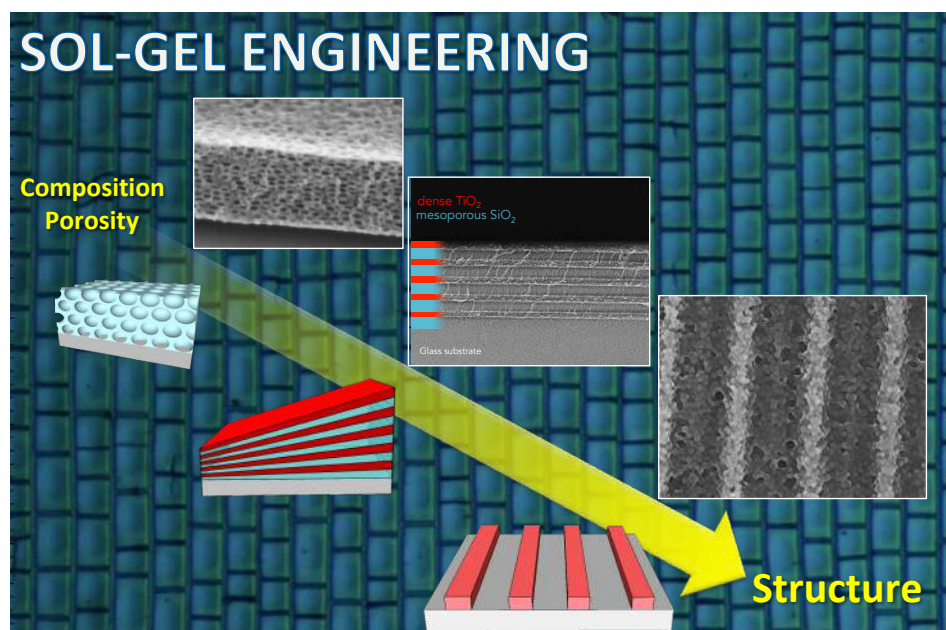
## Abstract

For several decades, the sol-gel process allows the fabrication of functional materials through the strong coupling between materials chemistry and advanced processing. This branch of material's science is generally associated to the formation of oxide and hybrid materials obtained through a transition between a sol and a gel. Engineering the sol-gel process to extend same principles to other classes of materials is an emerging and promising research line. These aspects will be illustrated in this article by reviewing the successful case of optical materials with tunable structural colors. It will be shown that sol-gel transition from molecular or colloidal building blocks results in optical materials with great diversity in structure and composition such as oxide, hybrid or, Metal Organic Frameworks. Applicative examples will be provided including photocatalytic, "invisible" and anti-reflective coatings, graded photonic mirrors and 2D photonic sensors.

## Keywords

Sol-gel, MOFs, anti-reflection, crack self-assembly, diffraction gratings

## Graphical abstract



# 1. Introduction

## 1.1. Better Ceramics through Chemistry, 30 years after

The legacy of Donald R. Ulrich concerns the rise of the sol-gel field that he promoted in the famous series of symposiums called "Better Ceramic through Chemistry"[1,2] These events marked the beginning of the sol-gel community[3]. At the time, he pioneered the so-called "ultrastructure processing" of glass-ceramic materials by chemical strategies. This approach was described by D. Ulrich in 1988, as chemical processing at the sub-micrometric scale based on molecular manipulation of various types of sols, gels, and organometallic precursors at low temperature that could eventually be converted to ceramic materials at more elevated temperatures[4]. After more than 30 years from Ulrich's perspective article, most of the key advantages of sol-gel in term of chemistry and processing are still valid today.[3] Since the very beginning, the sol-gel process is ideally suited to fabricate inorganic and hybrid materials with great control of the compositions, structuration and unbeaten versatility.[5] Notably, such inorganic polymerization at low temperature combined with soft-templating allowed the fabrication of mesostructured and mesoporous materials [6-8]. From a technological point of view, the sol-gel process undergoes a liquid-solid rheological transition allowing shaping of the inorganic materials very much as polymers [9]. The processing step can be applied at different stages: for instance thin films can be obtained by deposition process from the liquid sol [10,11]. Replication, molding, templating or shaping of inorganic materials are usually carried out on more viscous systems just before gelification [9]. Different shaping processes can also be combined giving rise to materials with sophisticated architecture that can be key components for new applications, at least for sol-gel materials.

Yet the concept of sol-gel goes now beyond the synthesis of ceramic materials by inorganic polymerization. In the last years, new sol-gel processing routes are emerging. According to IUPAC, the sol-gel is "a process through which a network is formed from solution by a progressive change of liquid precursor(s) into a sol, to a gel, and in most cases finally to a dry network"[12,13] . Consequently, in addition to what is generally assumed, materials obtained by a sol-gel process are not exclusively oxides or ceramics but can be carbon-based materials [14] or even Metal-Organic Frameworks (MOFs) [15]. This broader field, that can be defined as "sol-gel engineering"; it takes advantage of the 30 years old know-how of conventional sol-gel routes and emerging chemical/process engineering methods to extend those strategies to other class of materials.

In this article conventional and emerging sol-gel routes will be discussed by focusing on the successful case of optical coatings exhibiting structural colours. This is not meant to be a comprehensive review on the field of photonic sol-gel materials, excellent reviews can be found in the literature [16]. Rather, this article is an overview on recent accomplishments on how structural colours in thin films can be engineered to tackle some applicative challenges by mastering the sol-gel process starting from molecular but also from colloidal building blocks.

## 1.2. Sol-gel Optical Coating: Old Topic, Countless Opportunities

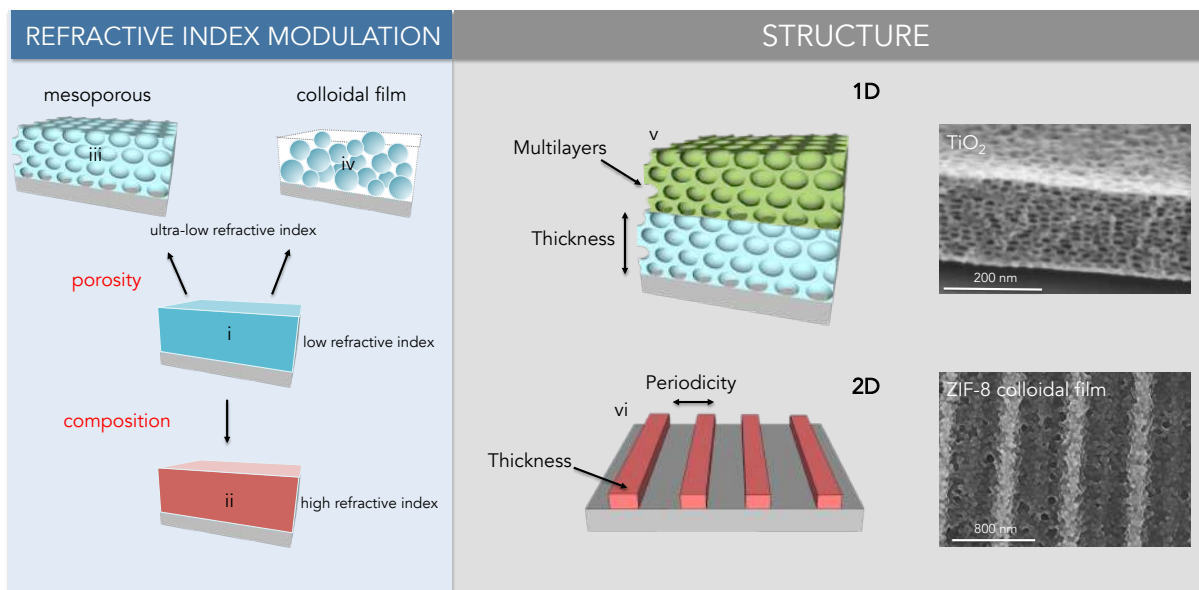


**Figure 1** Conceptual illustration of the some general strategies associated to the molecular design and construction of functional sol-gel derived coatings with tunable optical properties: (i) low refractive index material, (ii) high refractive index material, (iii) porous material, (iv) colloidal films (v) 1D interferential coatings (vi) 2D photonic systems.

Since the very beginning of its long history, sol-gel process was identified as a promising technology for optical applications [17]. More than two decades ago, J. Livage et. al. describe the potential of sol-gel as " the ability to go all the way from the molecular precursor to the product, allowing a better control of the whole process and the synthesis of "tailor-made" materials "[18] . Curiously, the sol-gel technology driven by industrial needs was maybe developed before the sol-gel science. The first example on sol-gel optical coatings dates back to 1930 with the patent deposited from Geffcken and Berger from Schott Glaswerke Company. It describes the fabrication of oxide layers from metal oxide precursors by dip-coating [19]. The first products appeared on the market in 1953 and large scale production in 1959 with automotive rear-view mirrors, later anti-reflection coatings and sunshielding windows were introduced using  $\text{TiO}_2$  and  $\text{SiO}_2$  layers [20].

Despite its old history, sol-gel process still offers countless possibility to modulate optical properties [5]. Let's consider the case of a thin film. The optical performances depend on a combination of the intrinsic properties of the material and its structure. The sol-gel processing alone does not change the intrinsic properties of the materials. However, it offer new chemical strategies to assemble materials having unique structure at different scales [20]. To introduce the following part, some general strategies associated to the molecular design of coatings with tunable optical properties in the visible range will be described (Figure 1).

Refractive index modulation can be achieved by tuning the composition or adding porosity. Those heterogeneities must remain in the sub-wavelength range in order to consider the material as an effective medium. Let's focus on the case of "transparent" dielectric material that is not absorbing in the considered wavelength range. The simplest case is illustrated in Figure 1i); it corresponds to a sol-gel derived dense film with low refractive index, made of silica for instance. The best way to tune the refractive index of the material consists in changing the material's composition by modifying the initial synthetic conditions.

For instance, among the sol-gel materials, amorphous  $\text{SiO}_2$  is considered a low refractive index material ( $n= 1.45$  at 550nm) while nanocrystalline  $\text{TiO}_2$  is a high refractive index material ( $n= 2.2-2.4$  at 550nm) widely used in optical devices (Figure 1ii). Mixing two (or more) oxides such as  $\text{SiO}_2$  and  $\text{TiO}_2$  allows precise tuning of the refractive index of the coatings. For instance, amorphous and crystalline optical films made of binary  $\text{SiO}_2\text{-TiO}_2$  can be obtained by co-condensation of Si and Ti oligomers [21]. Alternatively, nanocomposite networks with tunable optical density have been obtained by co-deposition of preformed  $\text{TiO}_2$  nanocrystals and  $\text{SiO}_2$  molecular precursors or particles [22].

The optical modulation of the refractive index can also be achieved by adding porosity in which the micro- or mesoporous layers can thus be seen as composite material composed by the inorganic phase and by air as illustrated in Figure 1(iii). Mesoporosity is formed from self-assembly of molecular or polymeric amphiphilic components coupled with polycondensation reactions or with other colloidal chemistry-based approaches [8,23]. The texture inducing process and the formation of the hybrid interface can be made by self-assembly of micelles, bridge hybrid precursors, lyotropic liquid crystals, or polymeric beads [24-28]. The porosity is obtained after the removal of the organic template by washing or by thermal treatment. Alternatively, nanoporous layers can be obtained by colloidal films (Figure 1iv), in which the void is localized in the inter-particles space. Colloids themselves can be porous as in the case of Metal-Organic Frameworks.

A unique feature of sol-gel materials is the capability to be shaped/combined periodically in order to "mold the flow of light" [29] by inducing structural colours thanks to interference, diffraction and photonic phenomena. In this category one can cite several kind of devices such 1D and 2D systems made, for example, of mesoporous materials or colloidal materials such as nanometric Zeolitic imidazolate framework 8 (ZIF-8) as shown in Figure 1 v and vi respectively. Here the structural colour will depend not only of the refractive index of the components but also on their structure at a larger scale in terms of thickness, periodicity, stacking, etc.. This is an extremely active field as evidenced by many important contributions reported in the last years from several groups [30-33].

In the following section, some recent examples of functional optical films developed in our group will be reported in which the structural colours were suppressed or induced to achieve specific functionalities.

## 2. Suppressing Structural Colours

### 2.1. "Invisible" photocatalytic coatings on glass

Glass is an outstanding material, massively employed in everyday life such as in optical devices, architecture, automobile and arts. Additional functionalities can be integrated in standard glasses by functional coatings. One topic of great interest concerns design multifunctional coatings on glass exhibiting several properties such as photoactivity, anti-reflectivity, mechanical resistance and, more even importantly, "invisibility". Why? Let's first illustrate this property with the example of photocatalytic coatings.

Photocatalytic coatings allow the glass surface to be "active" enabling decomposition of organic species under light irradiation [34,35]. They can be used for: (i) their self-cleaning capabilities, to decompose non-volatile organic species from the surface[36] preserving the surface appearance or (ii) air depollution of volatile organic compounds especially if they are

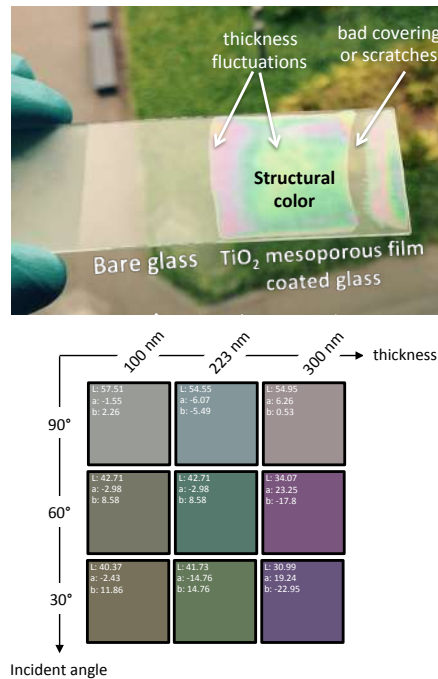


**Figure 2** Structural colours on glass: (top) photograph and (bottom) simulation as function of the thickness and angle. Adapted from [37]

odorous and harmful [38-40]. To be applied on glass, an ideal coating must be highly photoactive with high surface area and with good mechanical, chemical and thermal stability. TiO<sub>2</sub> based mesoporous coatings have been considered as most serious candidates [41,42]. Optical quality nanocrystalline TiO<sub>2</sub> mesoporous films can be obtained by sol-gel process in presence of templating agents [43,44] and can be easily applied by liquid deposition techniques [45].

However, porous photocatalytic films have not been applied yet in real applications. One of the main issues is the esthetical appearance of the coated-glass [46,47]. As illustrated in Figure 2, when the refractive index of the coating differs from the one of glass, structural colours are observed due interference phenomena taking place at the air/coating/glass interfaces [48,49]. Here structural colours are not suitable for design conception in many applications especially for architectural windows or automobile windshields. This (un) esthetical effect is even more problematic when the coating's thickness is not homogenous over the surface provoking colour fluctuation visible by naked eye [5].

The "easiest way" to suppress the structural colors consists in matching the refractive index of glass all over the visible range of wavelengths. Due to the high refractive index of TiO<sub>2</sub> ( $n \approx 2.4$ ) compared to glass ( $n \approx 1.5$ ), one option to approach index-matching would consist in adding a low refractive index material, such as silica, in a TiO<sub>2</sub> porous network [50]. Mesoporous SiO<sub>2</sub> coatings containing preformed TiO<sub>2</sub> nanoparticles have been proposed by T. Gacoin's and later by Steiner's groups mainly to target photocatalytic properties [51,52] and anti-reflectivity.<sup>36</sup> However those interferential coatings always exhibit structural colours. In a first example, photoactive invisible coatings obtained by mixing TiO<sub>2</sub>, SiO<sub>2</sub> and air were designed by a rational approach based on simulation/experimental [37]. This approach can be described as follows: (i) measurement of the refractive index dispersion for each

component by spectroscopic ellipsometry; (ii) simulation of the reflected structural colours for different compositions by establishing 3-phases diagram (Figure 3); (iii) preparation of the “invisible coatings”. Guided by simulation, photocatalytic  $\text{TiO}_2\text{-SiO}_2$  mesoporous coatings were fabricated by one liquid deposition step process exploiting the evaporation induced self-assembled method using F127 block copolymer as an organic template mixed with  $\text{TiO}_2$  and  $\text{SiO}_2$  molecular precursors at various Ti/Si ratio. As revealed by Environmental Ellipsometric Porosimetry, Grazing-Incidence Small-Angle X-ray Scattering (GI-SAXS) and Grazing-Incidence Wide-Angle X-ray Scattering (GI-WAXS), addition of  $\text{SiO}_2$  on  $\text{TiO}_2$ -based coatings results in a progressive porous network reconfiguration from “open” grid-like structure to more “isolated” spherical pores. As shown in Figure 3, only a precise combination of composition (60% $\text{TiO}_2$ ,40% $\text{SiO}_2$ ) and porosity (40%vol) allows obtaining invisibility, improved mechanical stiffness and high photocatalytic activity [53].

This can be observed in Figure 3 (right) showing the transmission curves for different thicknesses of the “invisible” layers that are nearly identical to the one of the bare substrate (as opposed to a typical mesoporous titania). Starting from the experimental transmission curves, the simulated reflected colours on “invisible” coatings present no shade, with a low dependency towards coating thickness and incidence angle. This is an important advantage in terms of processing because it allows obtaining “esthetical” photocatalytic coatings even in the case of thickness fluctuation during deposition. Thus low cost, larger scale deposition processes such as spray-coating can be considered.

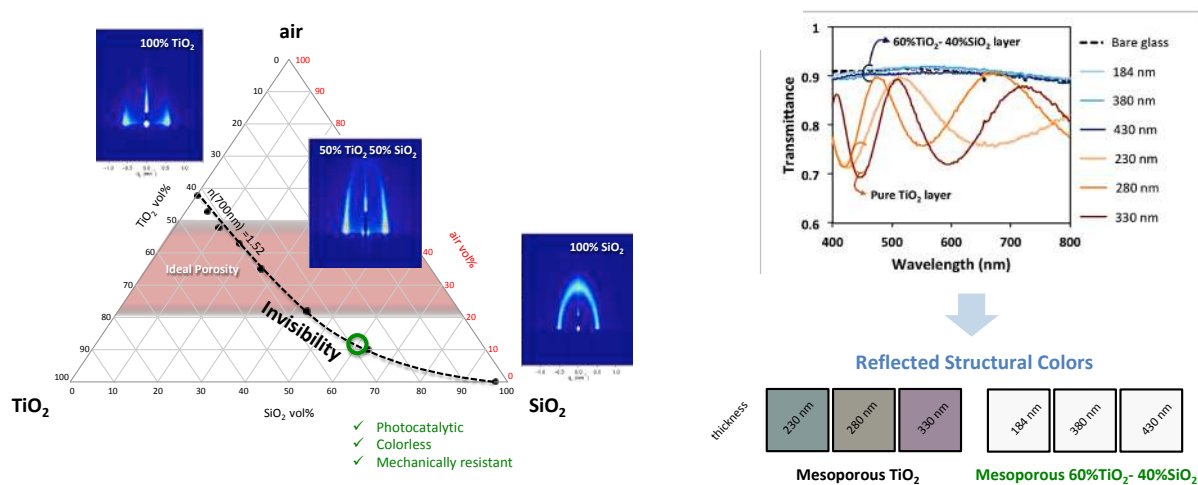


**Figure 3** (left) 3-phases diagram and GI-SAXS patterns to follow the evolution of the refractive index and mesostructure in  $\text{SiO}_2/\text{TiO}_2$  porous composites (right) transmittance curves and simulated reflected colour of the “invisible” coatings. Adapted from [37]

## 2.2. Anti-reflective and photocatalytic coatings on glass

While glass is usually characterized by a high transmittance, another optical effect occurring at the glass/air interface is a partial reflection of light due to the refractive index contrast between the two media. This reflection is not technically considered as a structural colour, but is a common drawback for optical devices such as solar cells, automobile windshield or glass lenses. How to suppress reflection from photocatalytic coatings? A first approach consists in developing a single TiO<sub>2</sub> based multifunctional layer. An anti-reflective self-cleaning film deposited on glass would require a refractive index around 1.25. As mentioned above, TiO<sub>2</sub> refractive index is high (2.2-2.4) and reducing refractive index can be achieved by "adding" a large volume of porosity. This is challenging because a highly porous network generally collapses during crystallisation. This issue was overcome by developing an anti-reflective and photocatalytic crystalline TiO<sub>2</sub> layer with refractive index down to 1.27 and a hierarchical porosity up to 80% vol [54]. The great stability of the porosity upon thermal induced crystallisation and template removal was attributed to the combined effects of the presence of silica in the inorganic phase (10% mol) and the use of templates with different dimensions ranging from a few nanometers to 50 nm (PB-PEO, Pluronic F17, and PEG) [53]. The transmittance spectrum of the coated glass is reported in Figure 3 showing a characteristic V-curve and a gain in transmitted light of more than 3% (at 500 nm). While this coating is extremely appealing for its photocatalytic properties it presents some issues to meet industrial requirements: (i) due to the high porous volume this coating is mechanically fragile and (ii) water can be uptaken at low relative humidity by capillary condensation into the hydrophilic porosity increasing the refractive index of the film [35].

To prepare anti-reflective, photo-catalytic coatings and avoid water condensation, approaches based on multi-coatings were developed [55]. One example of antireflective, water-repellent, self-cleaning and anti-fogging multilayer is shown in Figure 4. The system is composed of a stack of two layers: (i) a hydrophobic, anti-reflective bottom layer composed by a methylated mesoporous silica film exhibiting water repellency and durable optical properties; (ii) an hydrophilic TiO<sub>2</sub> patterned top-layer acting as anti-fogging and self-cleaning film due to the capability of anatase to UV-decompose organic compounds. The transmittance of the bilayer is plotted in Figure 4 together with the one of the ultraporous single layer detailed in previous example. While showing similar antireflective performances, the multilayer systems exhibit high mechanical, chemical and optical durability, making them serious candidates to be used as top antireflective coatings for photovoltaic cells or automobile for instance.



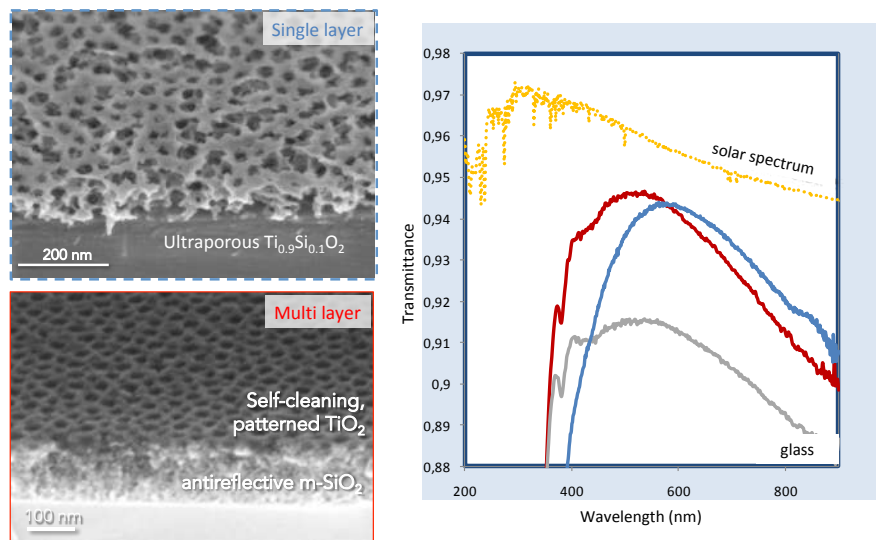


**Figure 4** Multifunctional photocatalytic anti-reflective coatings: single layer[54] vs multi layers strategies[55]

### 3. Tuning Structural Colours

#### 3.1. Graded 1D Photonic Crystals

To master the appearance of structural colours, the thickness of the coatings needs to be perfectly controlled. Spin-coating is widely used because it offers several advantages (single-side coating, low solution volume required). However, dip-coating is the first liquid deposition technique applied to sol-gel materials and probably the one that gives the best control in terms of thickness and evaporation rate. Several models have been proposed to predict the evolution of the thickness as respect to the withdrawal speed and temperature. At speeds above  $1 \text{ mm}\cdot\text{s}^{-1}$ , the thickness-speed relationship can be described by the Landau-Levich model [56]. In 2010, a new “capillary regime” was described at speed below  $0.1 \text{ mm s}^{-1}$  for sol-gel systems obtained by hydro-alcoholic solutions. In this case, the deposition is governed by the evaporation of the solvent at the meniscus that drives a convective flow of the solutes from the solution to the triple point. This phenomenon is better known as “coffee-ring effect” observed in the case of evaporating colloidal droplets and evidenced by Deegan in 1997 [57]. In this configuration, the final thickness is proportional to the withdrawal speed at the power  $-1$ . Between the capillary and draining regime, an intermediate regime is located between  $0.1$  and  $1 \text{ mm}\cdot\text{s}^{-1}$  where the minimal thickness is obtained. A global semi-empirical predictive model was proposed taking into account both capillary and draining regimes.

Once established simple semi-empirical rules governing dip-coating deposition, other contributions were reported in the following years [58-61]. One example is the development of a new method called “ dip coating in acceleration mode ” to fabricate surfaces with gradients of properties [62]. Indeed graded surfaces can be useful in many technological domains such as for controlled wetting, combinatorial studies, tunable optics, aerospace, etc. and, of course, to tune structural colours.

Fabrication of surfaces with gradient of optical properties is challenging. How dip-coating can help?

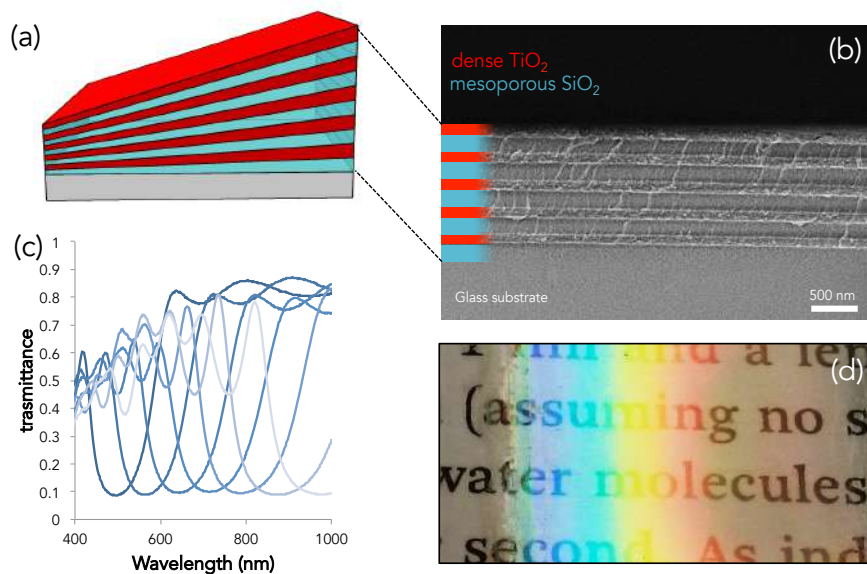


**Figure 5** (a) Graded 1D photonic crystals made by dip-coating in acceleration mode, (b) cross-section SEM, (c) transmittance as function of the lateral distance (d) photograph of the device. Adapted from [62]

As mentioned before in a conventional dip-coating process the substrate is withdrawn from a solution at a constant speed; the final thickness depends on the value of the latter withdrawal speed. Now, if the dip speed is dynamically increased during dip coating (by accelerating) one can theoretically obtain films with variable thickness along the dipping direction. The influence of the speed variation on the thickness profiles was investigated unveiling the important roles played by the evaporation rate and by the viscosity on the fluid draining-induced film formation. Through this study, a semi-experimental equation to obtain on-demand thickness profiles was established [62].

By exploiting the dip-coating in acceleration mode, several examples of graded devices could be demonstrated such as graded optical interferometry mirrors/filters, microfluidic channels with gradient in height, or surfaces with wettability gradient [62].

One interesting example concerns 1D photonic crystals. In general, they consist of an alternating, high and low refractive index dielectric multilayer stack. To obtain higher reflectivity, one should (i) increase the refractive index contrast between low and high refractive index layers and/or (ii) increase the number of layers (typically at least 4 pairs). As discussed above low refractive index materials are SiO<sub>2</sub> (or even mesoporous SiO<sub>2</sub>) while TiO<sub>2</sub> and ZrO<sub>2</sub> are often chosen as high refractive index materials. The optical thickness,  $nh$  of each layer equals  $\lambda/4$ , with  $\lambda$  being the wavelength for which Bragg reflection occurs,  $n$  the refractive index of the materials and  $h$  the layer thickness [16]. The position of the so-called 'stop-band' can be tuned by controlling the thickness of the layers.

Figure 5 illustrates a 1D photonic crystal exhibiting a controlled lateral gradient in photonic stop-band. The system is made of 5 pairs of alternated low and high refractive index layers based on mesoporous SiO<sub>2</sub> and dense TiO<sub>2</sub> (Figure 5(a)). Both materials have been processed in order to obtain linear gradients.

A cross-section view of the multi-stack is displayed in the SEM micrograph in Figure 5b. The optical device on glass substrate acts as graded reflectors as demonstrated by the optical

photo in Figure 5(d). In particular, Figure 5(c) shows the transmission data of the systems taken at various dipping distance. In this example, the photonic stop-band can be displaced over a very wide range of wavelengths (from 470 to 960 nm) without variation in the minimum transmittance values (less than 10%). This kind of device can be potentially used as versatile optical filter or mirror in which the stop-band position can be easily tuned from UV to the Near InfraRed domains (depending on the absorption limits of all components) by simply displacing the light beam position over the surface. The same concept can be generalized to a wide range of lower or higher wavelengths. However fabrication of thicker stacks in the IR is more challenging due to the formation of cracks during annealing.

### *3.2. MOF-based Colloidal 2D Diffraction Gratings*

As mentioned above, sol-gel process is not limited to molecular inorganic precursors undergoing inorganic polymerizations. Gelation of colloidal solutions can also be considered as a sol-gel process. Consequently "sol-gel engineering" to tune structural colours can be extended to other hybrid colloidal materials such as MOFs containing intrinsically micro-mesoporosity. Periodic materials exhibiting tunable structural colours can also thus be envisioned as photonic vapour sensors for instance. In this regard, the targeted materials are nanoporous materials such as sol-gel based micro or mesoporous materials or/and MOFs. Porous photonic structures are appealing for sensing applications,[63] for which the optical output relies on the change of refractive index in response to the analyte adsorption into the porosity [64,65]. Common photonic structures are Photonic Crystals made of periodic variation of optical density commonly in 1 or 3 dimensions. Considering the case of MOFs, some recent works demonstrated the integration of MOFs into photonic components such as thin films, [64,65] Fabry-Pérot,[66] 1D Bragg stacks,[67-69] or 3D colloidal crystals [70]. In all these examples, a gaseous pollutant uptaken into the pores provokes a change in the reflected colour.

One emerging class of photonic devices consists in the 2D porous Diffraction Gratings. They are optical components with a periodic structure, which splits and diffracts light into several beams travelling in different directions.

The sensing method relies on the evaluation of the diffraction intensity change, induced by the MOF refractive index variation, which can be simply detected by a CCD camera, as those integrated in simple smart-phones. Thanks to the angular dispersion generated by the grating, it is possible to monitor the intensity change on all the wavelengths simultaneously with a camera. The example in Figure 6 shows a smart-phone assisted detection (at one wavelength) using ZIF-8 colloidal films as sensing materials. This MOF is particularly appealing since its porosity is hydrophobic and uptakes selectively organic pollutant but not water vapors (the main interferent in atmospheric sensing). In this specific example this selectivity was exploited to detect styrene vapors in humid atmosphere (a common « practical » problem in the chemical industry). The optical transduction was ensured by diffraction gratings based on TiO<sub>2</sub>/ZIF-8 heterostructures obtained by direct Nanoimprinting Lithography of sol-gel films [71,72]. The detection of styrene down to 57ppm could be performed by a simple CCD camera and, interestingly, was based on the dynamic variation of diffraction intensity (rather than the absolute value) [50].



### 3.3. Photonic Cracks

One of the common issues while fabricating colloidal films from liquid solutions is the formation of cracks. Crack nucleation and propagation in thin films is widely studied because of its ubiquitous appearance in gelation processes of colloidal suspensions occurring during drying in both natural systems such as mud or in artificial materials such as paint or nanoparticles films.

During drying, the colloidal gels slowly desiccate and shrink leading to an accumulation of internal stress that is released by crack nucleation and propagation. Noteworthy, in some cases, the propagation of the cracks throughout the film is not totally random; specific orientation and a structure composed of polyhedral patterns arises. Because the crack formation originates from the evaporation of the solvent from the suspension, drying in controlled conditions at slow evaporation rates such as the one encountered in the capillary regime (the "coffee ring" effect), gives a better self-organization of the cracks.

A promising approach consists in harnessing the formation of cracks in "coffee rings" by dip-coating in the capillary regime. The final goal is to develop a straightforward patterning method. Figure 8 (top-left) schemes the dip-coated assisted crack self-assembly approach. In the process, the substrate is first dipped into colloidal solution and withdrawn at low speed. During dip coating, three characteristic zones can be identified. The colloidal solution is located below the triple line. Just above the triple line, the nanoparticles form a "wet" colloidal gel made of percolating particles and filled with the solvent. Internal stresses start to accumulate because of the shrinkage provoked by solvent removal. In the "wet gel", regularly spaced cracks appear to release the evaporation-induced stress and then propagate perpendicularly to the drying line. Above the drying line, the solvent evaporates completely leaving a "dry-gel". The dried film is thus composed by an oriented, regularly spaced, microgrooves arrays.

As discussed, the fabrication of diffraction gratings can be done by approaches based on lithographic methods. While providing an excellent control, all these methods present critical drawbacks related to substrate geometry, scalability, versatility and/or cost.

Alternatively crack self-assembly can be an appealing « bottom-up » strategy to fabricate such 2D patterned structures. It has been demonstrated that Metal-Organic Framework colloidal films can be crack-patterned during dip-coating deposition where the crack propagation is oriented by the evaporation front [76].

Figure 8 (top-right) show an optical micrograph of the final systems that is composed of is a colloidal film composed by oriented, regularly spaced, brick-like micropatterns.

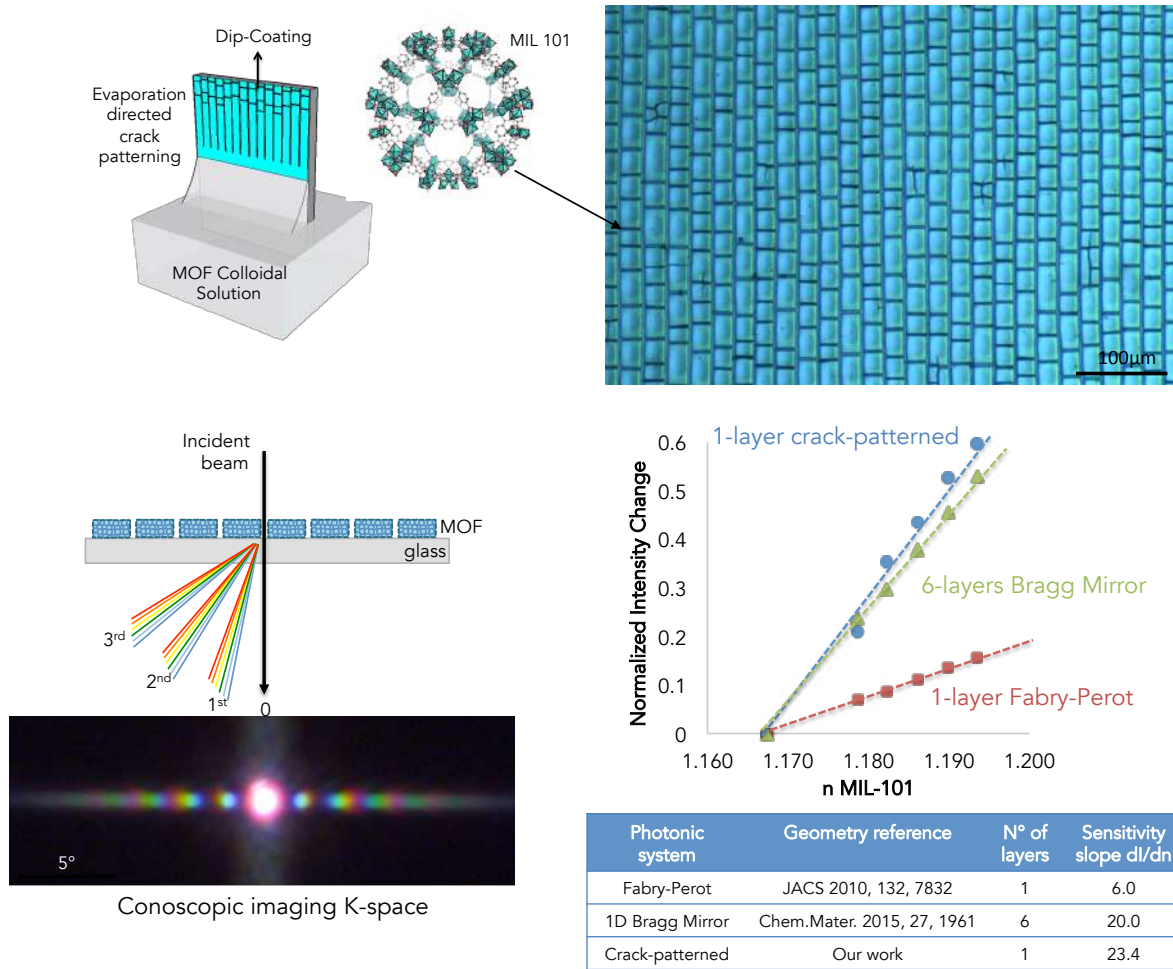


**Figure 8** Evaporation Directed Crack Assembly of colloidal MOFs to fabricated photonic sensors. Adapted from [76]

Due to this high degree of order of the periodic structure in the direction perpendicular to the drying line, the crack-patterned MOF film diffracts light acting as diffraction grating. This dispersive capability of a crack-patterned MIL-101 films coated on glass was proved by Conoscopic Imaging in transmission mode performed using a microscope equipped with a Bertrand lens (Figure 8 bottom-left). Taking advantage of the high porosity and of the selective sorption properties of MIL-101(Cr) and on the versatility of the crack-patterning process, a diffraction grating vapor sensors was developed. The signal transduction relies on the change of refractive index  $\Delta n$  in response to the vapor adsorption into the porosity as predicted by simple models proposed by Whitesides and co-workers [77,78] for gratings made of arrays of lines and is given in Equation (1):

$$\varphi = \frac{2\pi h(n_{MOF} - n_{air})}{\lambda} \quad (1)$$

with  $\varphi$  representing the phase difference created when light passes through the MOF-based crack-patterns. The phase difference depends on the light wavelength  $\lambda$ , on the thickness  $h$ , and on the refractive index contrast between the colloidal MOF film ( $n_{MOF}$ ) and the atmosphere ( $n_{air}=1$ ).

The first order diffracted intensity can be deduced by Equation (2)

$$I_1 = \frac{2(1 - \cos\varphi)}{\pi^2} \quad (2)$$

As a consequence, knowing  $n$  and  $h$  evolutions of the MOF material, the sensor response ( $dl_1/dn$ ) can be maximized simply by controlling the thickness  $h$ . This property of diffraction gratings allows fabrication of sensors with “on-demand”, enhanced sensitivity depending on the detection range [76].

The sensitivity performance ( $dl_1/dn$ ) of the crack-patterned sensor has been compared through optical simulation to MIL-101 based Fabry-Perot and Bragg-Mirror sensors by adapting geometry and structural parameters from literature data and considering their best sensing configurations [66,69]. As detailed in Figure 7 (bottom-right), for a value of thickness that maximizes  $dl_1/dn$ , the crack-patterned sensor shows the best sensitivity that is comparable (and even higher) to the Bragg-Mirror system; this is remarkable considering that a Bragg-Mirror requires 6 steps of deposition of 2 different materials while crack-patterning can be realized in a single step. Beyond these performances, this study represents the first example of cracks harnessing for photonic applications with important implications from the applicative point of view.

#### 4. Conclusions and perspectives

In this contribution, I reviewed some recent accomplishments in the fabrication of functional coatings with tuneable structural colours fabricated through “engineering” sol-gel strategies to conventional and emerging materials. In particular, suppression or appearance of structural colours was obtained by controlling the interplay between intrinsic optical properties of the materials and their structure. In this context, it was evidenced that sol-gel processing of (mesoporous) oxides from conventional molecular routes is perfectly suited to control composition, porosity and structure, especially when coupled with nanofabrication methods. This is a mature field that is now ready to solve great issues for challenging optical applications. For instance, an approach based on the direct nanoimprinting of sol-gel films has recently permitted to design a light trapping device exhibiting extremely high efficacy in ultrathin solar cells [79].

Importantly, following the same principles, sol-gel processing can be exploited starting from colloidal building blocks to shape photonic materials, by crack self-assembly for instance. The example of colloidal Metal-Organic Framework photonic surfaces was shown as practical case to prepare vapour sensors. This is extremely interesting for the evolution of the sol-gel field and to extend these strategies to other class of materials. For instance, in a recent article, simultaneous colloidal and molecular gelation has been exploited to fabricate highly porous metallic structures [80]. In general, it is believed that taking advantage of the versatility of the sol-gel process by extending the composition threshold (beyond oxides) is an exciting future research line for the field.

#### Acknowledgments

Sorbonne Université, CNRS and Collège de France are acknowledged. M. F. gratefully acknowledges all the co-authors of the works described in this article. M. F. acknowledges the funding from the European Research Council (ERC) under European Union's Horizon 2020 Programme (Grant Agreement no. 803220, TEMPORE) .

## Conflict of interest

The author declares that he has no conflict of interest.

## References

1. Ulrich DR (1988) Better Ceramics Through Chemistry. In: Laine RM (ed) Transformation of Organometallics into Common and Exotic Materials: Design and Activation. Springer Netherlands, Dordrecht, pp 207-235. doi:10.1007/978-94-009-1393-6\_19
2. Brinker CJ, Clark DE, Ulrich DR Better ceramics through chemistry II. In: MRS Symposium Proceedings, 1986.
3. Faustini M, Nicole L, Ruiz-Hitzky E, Sanchez C (2018) History of Organic–Inorganic Hybrid Materials: Prehistory, Art, Science, and Advanced Applications. *Advanced Functional Materials* 28 (27):1704158. doi:10.1002/adfm.201704158
4. Ulrich DR (1988) Prospects of sol-gel processes. *Journal of Non-Crystalline Solids* 100 (1):174-193. doi:https://doi.org/10.1016/0022-3093(88)90015-4
5. Faustini M, Grosso D, Boissiere C, Backov R, Sanchez C (2014) "Integrative sol-gel chemistry": a nanofactory for materials science. *Journal of Sol-Gel Science and Technology* 70 (2):216-226. doi:10.1007/s10971-014-3321-9
6. Yanagisawa T, Shimizu T, Kuroda K, Kato C (1990) The preparation of alkyltriethylammonium–kaneinite complexes and their conversion to microporous materials. *Bulletin of the Chemical Society of Japan* 63 (4):988-992
7. Beck JS, Vartuli JC, Roth WJ, Leonowicz ME, Kresge CT, Schmitt KD, Chu CTW, Olson DH, Sheppard EW, McCullen SB, Higgins JB, Schlenker JL (1992) A new family of mesoporous molecular sieves prepared with liquid crystal templates. *Journal of the American Chemical Society* 114 (27):10834-10843. doi:10.1021/ja00053a020
8. Ceratti DR, Faustini M, Sinturel C, Vayer M, Dahirel V, Jardat M, Grosso D (2015) Critical effect of pore characteristics on capillary infiltration in mesoporous films. *Nanoscale* 7 (12):5371-5382
9. Faustini M, Boissiere C, Nicole L, Grosso D (2014) From Chemical Solutions to Inorganic Nanostructured Materials: A Journey into Evaporation-Driven Processes. *Chemistry of Materials* 26 (1):709-723. doi:10.1021/cm402132y
10. Brinker CJ, Frye GC, Hurd AJ, Ashley CS (1991) Fundamental of sol-gel dip-coating *Thin Solid Films* 201 (1):97-108. doi:10.1016/0040-6090(91)90158-t
11. Faustini M, Drisko GL, Boissiere C, Grosso D (2014) Liquid deposition approaches to self-assembled periodic nanomasks. *Scripta Materialia* 74:13-18. doi:10.1016/j.scriptamat.2013.07.029
12. Alemán JV, Chadwick AV, He J, Hess M, Horie K, Jones RG, Kratochvíl P, Meisel I, Mita I, Moad G, Penczek S, Stepto RFT (2007) Definitions of terms relating to the structure and processing of sols, gels, networks, and inorganic-organic hybrid materials (IUPAC



- Recommendations 2007). Pure and Applied Chemistry, vol 79.  
doi:10.1351/pac200779101801
13. Innocenzi P The sol to gel transition. Springer,
  14. Fellingner T-P (2017) Sol-gel carbons from ionothermal syntheses. Journal of Sol-Gel Science and Technology 81 (1):52-58. doi:10.1007/s10971-016-4115-z
  15. Tian T, Zeng Z, Vulpe D, Casco ME, Divitini G, Midgley PA, Silvestre-Albero J, Tan J-C, Moghadam PZ, Fairen-Jimenez D (2018) A sol-gel monolithic metal-organic framework with enhanced methane uptake. Nature Materials 17 (2):174-179.  
doi:10.1038/nmat5050
  16. Almeida RM, Portal S (2003) Photonic band gap structures by sol-gel processing. Current Opinion in Solid State and Materials Science 7 (2):151-157
  17. Dislich H, Hinz P (1982) Proceedings of the International Workshop on Glasses and Glass Ceramics from Gels History and principles of the sol-gel process, and some new multicomponent oxide coatings. Journal of Non-Crystalline Solids 48 (1):11-16.  
doi:[http://dx.doi.org/10.1016/0022-3093\(82\)90242-3](http://dx.doi.org/10.1016/0022-3093(82)90242-3)
  18. Livage J, Henry M, Sanchez C (1988) Sol-gel chemistry of transition metal oxides. Progress in Solid State Chemistry 18 (4):259-341. doi:[http://dx.doi.org/10.1016/0079-6786\(88\)90005-2](http://dx.doi.org/10.1016/0079-6786(88)90005-2)
  19. Berger G (1939).
  20. Naudin G, Ceratti DR, Faustini M (2017) Sol-Gel Derived Functional Coatings for Optics. In: Sol-Gel Materials for Energy, Environment and Electronic Applications. Springer, pp 61-99
  21. Louis B, Krins N, Faustini M, Grosso D (2011) Understanding Crystallization of Anatase into Binary SiO<sub>2</sub>/TiO<sub>2</sub> Sol-Gel Optical Thin Films: An in Situ Thermal Ellipsometry Analysis. The Journal of Physical Chemistry C 115 (7):3115-3122.  
doi:10.1021/jp109653p
  22. Lee D, Rubner MF, Cohen RE (2006) All-Nanoparticle Thin-Film Coatings. Nano Letters 6 (10):2305-2312. doi:10.1021/nl061776m
  23. Brigo L, Faustini M, Pistore A, Kang HK, Ferraris C, Schutzmann S, Brusatin G (2016) Porous inorganic thin films from bridged silsesquioxane sol-gel precursors. Journal of Non-Crystalline Solids 432:399-405
  24. Sanchez C, Boissiere C, Cassaignon S, Chaneac C, Durupthy O, Faustini M, Grosso D, Laberty-Robert C, Nicole L, Portehault D, Ribot F, Rozes L, Sassoie C (2014) Molecular Engineering of Functional Inorganic and Hybrid Materials. Chemistry of Materials 26 (1):221-238. doi:10.1021/cm402528b
  25. Soler-Illia G, Azzaroni O (2011) Multifunctional hybrids by combining ordered mesoporous materials and macromolecular building blocks. Chemical Society Reviews 40 (2):1107-1150. doi:10.1039/c0cs00208a
  26. Faustini M, Vayer M, Marmiroli B, Hillmyer M, Amenitsch H, Sinturel C, Grosso D (2010) Bottom-up Approach toward Titanosilicate Mesoporous Pillared Planar Nanochannels for Nanofluidic Applications. Chemistry of Materials 22 (20):5687-5694.  
doi:10.1021/cm101502n
  27. Faustini M, Giraud M, Jones D, Rozière J, Dupont M, Porter TR, Nowak S, Bahri M, Ersen O, Sanchez C (2019) Hierarchically Structured Ultraporous Iridium - Based Materials: A Novel Catalyst Architecture for Proton Exchange Membrane Water Electrolyzers. Advanced Energy Materials 9 (4):1802136
  28. Brinker CJ, Lu YF, Sellinger A, Fan HY (1999) Evaporation-induced self-assembly: Nanostructures made easy. Advanced Materials 11 (7):579-+. doi:10.1002/(sici)1521-4095(199905)11:7<579::aid-adma579>3.0.co;2-r

29. Joannopoulos JD, Johnson SG, Winn JN, Meade RD (2008) Photonic Crystals Molding the Flow of Light Second Edition Introduction. Photonic Crystals: Molding the Flow of Light, 2nd Edition:1-5
30. Yakovlev AV, Milichko VA, Vinogradov VV, Vinogradov AV (2016) Inkjet color printing by interference nanostructures. ACS nano 10 (3):3078-3086
31. Gazoni RM, Bellino MG, Fuertes MC, Giménez G, Soler-Illia GJAA, Ricci MLM (2017) Designed nanoparticle–mesoporous multilayer nanocomposites as tunable plasmonic–photonic architectures for electromagnetic field enhancement. Journal of Materials Chemistry C 5 (14):3445-3455
32. Checcucci S, Bottein T, Gurioli M, Favre L, Grosso D, Abbarchi M (2019) Multifunctional Metasurfaces Based on Direct Nanoimprint of Titania Sol–Gel Coatings. Advanced Optical Materials 7 (10):1801406
33. England GT, Russell C, Shirman E, Kay T, Vogel N, Aizenberg J (2017) The optical Janus effect: Asymmetric structural color reflection materials. Advanced Materials 29 (29):1606876
34. Banerjee S, Dionysiou DD, Pillai SC (2015) Self-cleaning applications of TiO<sub>2</sub> by photo-induced hydrophilicity and photocatalysis. Applied Catalysis B: Environmental 176–177:396-428. doi:<http://dx.doi.org/10.1016/j.apcatb.2015.03.058>
35. Li R, Faustini M, Boissiere C, Grosso D (2014) Water Capillary Condensation Effect on the Photocatalytic Activity of Porous TiO<sub>2</sub> in Air. Journal of Physical Chemistry C 118 (31):17710-17716. doi:10.1021/jp5046468
36. Paz Y, Luo Z, Rabenberg L, Heller A (1995) PHOTOOXIDATIVE SELF-CLEANING TRANSPARENT TITANIUM-DIOXIDE FILMS ON GLASS. J Mater Res 10 (11):2842-2848. doi:10.1557/jmr.1995.2842
37. Li R, Boudot M, Boissière C, Grosso D, Faustini M (2017) Suppressing Structural Colors of Photocatalytic Optical Coatings on Glass: The Critical Role of SiO<sub>2</sub>. ACS Applied Materials & Interfaces 9 (16):14093-14102. doi:10.1021/acsami.7b02233
38. Maggos T, Bartzis JG, Liakou M, Gobin C (2007) Photocatalytic degradation of NO<sub>x</sub> gases using TiO<sub>2</sub>-containing paint: A real scale study. J Hazard Mater 146 (3):668-673. doi:10.1016/j.jhazmat.2007.04.079
39. Ao CH, Lee SC, Yu JZ, Xu JH (2004) Photodegradation of formaldehyde by photocatalyst TiO<sub>2</sub>: effects on the presences of NO, SO<sub>2</sub> and VOCs. Applied Catalysis B-Environmental 54 (1):41-50. doi:10.1016/j.apcatb.2004.06.004
40. Ao CH, Lee SC, Mak CL, Chan LY (2003) Photodegradation of volatile organic compounds (VOCs) and NO for indoor air purification using TiO<sub>2</sub>: promotion versus inhibition effect of NO. Applied Catalysis B-Environmental 42 (2):119-129. doi:10.1016/s0926-3373(02)00219-9
41. Li W, Wu Z, Wang J, Elzatahry AA, Zhao D (2014) A Perspective on Mesoporous TiO<sub>2</sub> Materials. Chemistry of Materials 26 (1):287-298. doi:10.1021/cm4014859
42. Yang PD, Zhao DY, Margolese DI, Chmelka BF, Stucky GD (1999) Block copolymer templating syntheses of mesoporous metal oxides with large ordering lengths and semicrystalline framework. Chemistry of Materials 11 (10):2813-2826. doi:10.1021/cm990185c
43. Soler-Illia GJAA, Angelome PC, Fuertes MC, Grosso D, Boissiere C (2012) Critical aspects in the production of periodically ordered mesoporous titania thin films. Nanoscale 4 (8):2549-2566. doi:10.1039/C2NR11817C
44. Du J, Lai XY, Yang NL, Zhai J, Kisailus D, Su FB, Wang D, Jiang L (2011) Hierarchically Ordered Macro-Mesoporous TiO<sub>2</sub>-Graphene Composite Films: Improved Mass Transfer,

- Reduced Charge Recombination, and Their Enhanced Photocatalytic Activities. *ACS Nano* 5 (1):590-596. doi:10.1021/nn102767d
45. Ceratti DR, Louis B, Paquez X, Faustini M, Grosso D (2015) A New Dip Coating Method to Obtain Large-Surface Coatings with a Minimum of Solution. *Adv Mater* 27 (34):4958-+. doi:10.1002/adma.201502518
46. Fattakhova-Rohlfing D, Zaleska A, Bein T (2014) Three-Dimensional Titanium Dioxide Nanomaterials. *Chemical Reviews* 114 (19):9487-9558. doi:10.1021/cr500201c
47. Stathatos E, Lianos P, Falaras P, Siokou A (2000) Photocatalytically deposited silver nanoparticles on mesoporous TiO<sub>2</sub> films. *Langmuir* 16 (5):2398-2400. doi:10.1021/la981783t
48. Young T (1802) The Bakerian lecture: On the theory of light and colours. *Philosophical transactions of the Royal Society of London* 92:12-48
49. Kubota H (1950) On the Interference Color of Thin Layers on Glass Surface. *Journal of the Physical Society of Japan* 5 (1):10-14. doi:10.1143/JPSJ.5.10
50. Dong W, Sun Y, Lee CW, Hua W, Lu X, Shi Y, Zhang S, Chen J, Zhao D (2007) Controllable and Repeatable Synthesis of Thermally Stable Anatase Nanocrystal-Silica Composites with Highly Ordered Hexagonal Mesostructures. *Journal of the American Chemical Society* 129 (45):13894-13904. doi:10.1021/ja073804o
51. Allain E, Besson S, Durand C, Moreau M, Gacoin T, Boilot JP (2007) Transparent Mesoporous Nanocomposite Films for Self - Cleaning Applications. *Advanced Functional Materials* 17 (4):549-554
52. Guldin S, Kohn P, Stefik M, Song J, Divitini G, Ecarla F, Ducati C, Wiesner U, Steiner U (2013) Self-Cleaning Antireflective Optical Coatings. *Nano Letters* 13 (11):5329-5335. doi:10.1021/nl402832u
53. Grosso D, Soler-Illia GJdAA, Crepaldi EL, Cagnol F, Sinturel C, Bourgeois A, Brunet-Bruneau A, Amenitsch H, Albouy PA, Sanchez C (2003) Highly Porous TiO<sub>2</sub> Anatase Optical Thin Films with Cubic Mesostructure Stabilized at 700 °C. *Chemistry of Materials* 15 (24):4562-4570. doi:10.1021/cm031060h
54. Faustini M, Grenier A, Naudin G, Li R, Grosso D (2015) Ultraporous nanocrystalline TiO<sub>2</sub>-based films: synthesis, patterning and application as anti-reflective, self-cleaning, superhydrophilic coatings. *Nanoscale* 7 (46):19419-19425. doi:10.1039/C5NR06466J
55. Faustini M, Nicole L, Boissiere C, Innocenzi P, Sanchez C, Grosso D (2010) Hydrophobic, Antireflective, Self-Cleaning, and Antifogging Sol-Gel Coatings: An Example of Multifunctional Nanostructured Materials for Photovoltaic Cells. *Chemistry of Materials* 22 (15):4406-4413. doi:10.1021/cm100937e
56. C.J. Brinker AJH, P.R. Schunk, G.C. Frye and C.S. Ashley (1992) Review of sol-gel thin film formation. *Journal of non-crystalline solids* 147:13
57. Deegan RD, Bakajin O, Dupont TF, Huber G, Nagel SR, Witten TA (1997) Capillary flow as the cause of ring stains from dried liquid drops. *Nature* 389 (6653):827-829
58. Bindini E, Naudin G, Faustini M, Grosso D, Boissière C (2017) Critical Role of the Atmosphere in Dip-Coating Process. *The Journal of Physical Chemistry C* 121 (27):14572-14580. doi:10.1021/acs.jpcc.7b02530
59. Faustini M, Grosso D (2016) Self-assembled inorganic nanopatterns (INPs) made by sol-gel dip-coating: Applications in nanotechnology and nanofabrication. *Comptes Rendus Chimie* 19 (1-2):248-265. doi:<http://dx.doi.org/10.1016/j.crci.2015.05.011>
60. Faustini M, Capobianchi A, Varvaro G, Grosso D (2012) Highly Controlled Dip-Coating Deposition of fct FePt Nanoparticles from Layered Salt Precursor into Nanostructured Thin Films: An Easy Way To Tune Magnetic and Optical Properties. *Chemistry of Materials* 24 (6):1072-1079. doi:10.1021/cm2033492

61. Ceratti DR, Louis B, Paquez X, Faustini M, Grosso D (2015) A New Dip Coating Method to Obtain Large-Surface Coatings with a Minimum of Solution. *Advanced Materials* 27 (34):4958-4962. doi:10.1002/adma.201502518
62. Faustini M, Ceratti DR, Louis B, Boudot M, Albouy P-A, Boissiere C, Grosso D (2014) Engineering Functionality Gradients by Dip Coating Process in Acceleration Mode. *ACS Applied Materials & Interfaces* 6 (19):17102-17110. doi:10.1021/am504770x
63. Shekhah O, Liu J, Fischer RA, Woll C (2011) MOF thin films: existing and future applications. *Chem Soc Rev* 40 (2):1081-1106. doi:10.1039/c0cs00147c
64. Demessence A, Boissiere C, Grosso D, Horcajada P, Serre C, Ferey G, Soler-Illia G, Sanchez C (2010) Adsorption properties in high optical quality nanoZIF-8 thin films with tunable thickness. *Journal of Materials Chemistry* 20 (36):7676-7681. doi:10.1039/c0jm00500b
65. Demessence A, Horcajada P, Serre C, Boissiere C, Grosso D, Sanchez C, Ferey G (2009) Elaboration and properties of hierarchically structured optical thin films of MIL-101(Cr). *Chemical Communications* (46):7149-7151. doi:10.1039/b915011k
66. Lu G, Hupp JT (2010) Metal–Organic Frameworks as Sensors: A ZIF-8 Based Fabry–Pérot Device as a Selective Sensor for Chemical Vapors and Gases. *Journal of the American Chemical Society* 132 (23):7832-7833. doi:10.1021/ja101415b
67. Hinterholzinger FM, Ranft A, Feckl JM, Ruhle B, Bein T, Lotsch BV (2012) One-dimensional metal-organic framework photonic crystals used as platforms for vapor sorption. *Journal of Materials Chemistry* 22 (20):10356-10362. doi:10.1039/C2JM15685G
68. Hu Z, Tao C-a, Wang F, Zou X, Wang J (2015) Flexible metal-organic framework-based one-dimensional photonic crystals. *Journal of Materials Chemistry C* 3 (1):211-216. doi:10.1039/C4TC01501K
69. Ranft A, Niekkel F, Pavlichenko I, Stock N, Lotsch BV (2015) Tandem MOF-Based Photonic Crystals for Enhanced Analyte-Specific Optical Detection. *Chemistry of Materials* 27 (6):1961-1970. doi:10.1021/cm503640c
70. Lu G, Farha OK, Kreno LE, Schoenecker PM, Walton KS, Van Duyne RP, Hupp JT (2011) Fabrication of Metal-Organic Framework-Containing Silica-Colloidal Crystals for Vapor Sensing. *Adv Mater* 23 (38):4449-+. doi:10.1002/adma.201102116
71. Faustini M, Cattoni A, Peron J, Boissière C, Ebrard P, Malchère A, Steyer P, Grosso D (2018) Dynamic Shaping of Femtoliter Dew Droplets. *ACS Nano* 12 (4):3243-3252. doi:10.1021/acsnano.7b07699
72. Bottein T, Dalstein O, Putero M, Cattoni A, Faustini M, Abbarchi M, Grosso D (2018) Environment-controlled sol-gel soft-NIL processing for optimized titania, alumina, silica and yttria-zirconia imprinting at sub-micron dimensions. *Nanoscale* 10 (3):1420-1431. doi:10.1039/C7NR07491C
73. Echeverría JC, Faustini M, Garrido JJ (2016) Effects of the porous texture and surface chemistry of silica xerogels on the sensitivity of fiber-optic sensors toward VOCs. *Sensors and Actuators B: Chemical* 222:1166-1174. doi:<http://dx.doi.org/10.1016/j.snb.2015.08.010>
74. Boudot M, Ceratti DR, Faustini M, Boissiere C, Grosso D (2014) Alcohol-Assisted Water Condensation and Stabilization into Hydrophobic Mesoporosity. *Journal of Physical Chemistry C* 118 (41):23907-23917. doi:10.1021/jp508372d
75. Boudot M, Cattoni A, Grosso D, Faustini M (2016) Ethanol–water co-condensation into hydrophobic mesoporous thin films: example of a photonic ethanol vapor sensor in humid environment. *Journal of Sol-Gel Science and Technology*:1-10. doi:10.1007/s10971-016-4084-2

76. Dalstein O, Gkaniatsou E, Sicard C, Sel O, Perrot H, Serre C, Boissière C, Faustini M (2017) Evaporation-Directed Crack-Patterning of Metal–Organic Framework Colloidal Films and Their Application as Photonic Sensors. *Angewandte Chemie International Edition* 56 (45):14011-14015. doi:10.1002/anie.201706745
77. Schueller OJA, Duffy DC, Rogers JA, Brittain ST, Whitesides GM (1999) Reconfigurable diffraction gratings based on elastomeric microfluidic devices. *Sensors and Actuators A: Physical* 78 (2):149-159
78. Grzybowski BA, Qin D, Whitesides GM (1999) Beam redirection and frequency filtering with transparent elastomeric diffractive elements. *Applied optics* 38 (14):2997-3002
79. Chen H-L, Cattoni A, De Lépinau R, Walker AW, Höhn O, Lackner D, Siefer G, Faustini M, Vandamme N, Goffard J (2019) A 19.9%-efficient ultrathin solar cell based on a 205-nm-thick GaAs absorber and a silver nanostructured back mirror. *Nature Energy* 4 (9):761-767
80. Odziomek M, Bahri M, Boissiere C, Sanchez C, Lassalle-Kaiser B, Zitolo A, Ersen O, Nowak S, Tard C, Giraud M, Faustini M, Peron J (2020) Aerosol synthesis of thermally stable porous noble metals and alloys by using bi-functional templates. *Materials Horizons*. doi:10.1039/C9MH01408J